

## Article

# Cyanide Bioremediation by *Bacillus subtilis* under Alkaline Conditions

César Julio Cáceda Quiroz <sup>1,\*</sup> , Gabriela de Lourdes Fora Quispe <sup>1,\*</sup> , Milena Carpio Mamani <sup>1</sup>,  
Gisela July Maraza Choque <sup>1</sup>  and Elisban Juani Sacari Sacari <sup>2</sup> 

<sup>1</sup> Laboratorio de Biorremediación, Facultad de Ciencias, Universidad Nacional Jorge Basadre Grohmann, Avenida Miraflores S/N, Ciudad Universitaria, Tacna 23003, Peru

<sup>2</sup> Centro de Energías Renovables de Tacna (CERT), Facultad de Ciencias, Universidad Nacional Jorge Basadre Grohmann, Avenida Miraflores S/N, Ciudad Universitaria, Tacna 23003, Peru

\* Correspondence: ccacedaq@unjbg.edu.pe (C.J.C.Q.); gforaq@unjbg.edu.pe (G.d.L.F.Q.)

**Abstract:** Cyanide (CN) is a toxic environmental pollutant generated by various industrial activities, necessitating the application of bioremediation techniques for its degradation. Biodegradation is a more cost-effective and environmentally friendly technique with high efficiency in CN removal. This study isolated cyanide-degrading bacteria from Tutupaca mining site soil from Tacna, Peru. *Bacillus subtilis* strain TT10s was selected for its exceptional capacity to rapidly and completely eliminate cyanide under alkaline conditions (pH 10.5), removing 1000 ppm cyanide within 48 h. A kinetic analysis revealed that the biodegradation follows second-order rate kinetics ( $k_2 = 0.08649 \text{ mg}/(\text{mg}\cdot\text{h})$ ,  $R^2 = 0.96622$ ), consistent with the literature attribution of the rate-limiting step to the inducible cyanide dihydratase enzyme, which converts cyanide into ammonia and formate via the Michaelis-Menten model. Fourier-transform infrared spectroscopy (FTIR) spectral analysis further corroborated this enzymatic mechanism, showing the disappearance of CN peaks coupled with the emergence of ammonia (NH) and formate (C=O) peaks. Quantitative kinetic modelling integrated with FTIR profiles and degradation curves implicates cyanide dihydratase as the key rate-controlling enzyme in alkaline cyanide biodegradation without the need for an extra carbon source, generating interest for future bioremediation applications in highly contaminated environments.

**Keywords:** bioremediation; cyanide; *Bacillus subtilis*



**Citation:** Cáceda Quiroz, C.J.; Fora Quispe, G.d.L.; Carpio Mamani, M.; Maraza Choque, G.J.; Sacari Sacari, E.J. Cyanide Bioremediation by *Bacillus subtilis* under Alkaline Conditions. *Water* **2023**, *15*, 3645. <https://doi.org/10.3390/w15203645>

Academic Editors: Shakeel Ahmad, Shicheng Zhang, Mujtaba Baqar and Eric Danso-Boateng

Received: 1 September 2023

Revised: 27 September 2023

Accepted: 6 October 2023

Published: 18 October 2023



**Copyright:** © 2023 by the authors. Licensee MDPI, Basel, Switzerland. This article is an open access article distributed under the terms and conditions of the Creative Commons Attribution (CC BY) license (<https://creativecommons.org/licenses/by/4.0/>).

## 1. Introduction

Cyanide is a highly toxic pollutant generated from industrial activities like electroplating [1], mining [2], the production of organic chemicals [3], and others.

Cyanide is extensively used in mining, and Peru is not immune to the environmental impacts of cyanide [4] due to it being extensively used for gold and copper extraction [5]. This has resulted in severe environmental impacts from cyanide spills [4], leaks [6], and the improper discharge of contaminated wastewater into rivers and lakes, which has been exacerbated by the Peruvian government declaring states of emergency in certain regions [7]. Conflicts have emerged over water quality and supply between mining companies and local communities throughout Peru, especially in agricultural regions dependent on clean water [8,9]. Peru has developed regulations on cyanide use and discharge limits [10]; however, the strict enforcement of these regulations is necessary to ensure their efficacy, as stakeholders may ignore them.

Studies have detected high levels of cyanide contamination in different rivers in Tumbes [11], Tacna [12,13], Amazonas [14], Piura [15], Arequipa [16,17], and other regions in Peru, likely originating from legal and illegal mining operations [18].

The Tacna region in Peru faces several environmental liabilities left behind by abandoned informal mines where various materials, including cyanide, were used for gold, copper, and sulfur processing, reaching concentrations of up to 92 mg/kg of free cyanide

in the Cano community [13]. These sites are located close to rivers, leading to risks of water contamination that could have negative effects on the environment and health of people consuming the polluted water [13].

The accumulation of cyanide in the environment poses risks to ecosystems and human health due to its ability to inhibit essential metalloenzymes [19,20]. Conventional physico-chemical methods for cyanide removal have limitations like high costs, secondary pollution, and the inability to completely destroy cyanide [21]. Bioremediation techniques using microbes provide a promising, eco-friendly solution to decontaminate cyanide-polluted sites and prevent further environmental damage [22,23]. A range of bacterial species have been studied for their ability to degrade cyanide, either as the sole source of nitrogen or co-metabolically with other substrates. Common cyanide-degrading bacteria include species from the genera *Pseudomonas*, *Bacillus*, *Klebsiella*, *Burkholderia*, and *Rhodococcus*. Within the *Pseudomonas* genus, *P. pseudoalcaligenes* [24], *P. fluorescens* [25], and *P. putida* [26] display cyanide removal capabilities. *Bacillus megaterium* [27], *B. subtilis* [28], *B. pumilus* [29], and *B. cereus* [30] strains have also been investigated. Other promising cyanide-degrading bacteria include *Klebsiella oxytoca* [31], *Burkholderia cepacia* [32], and *Rhodococcus* sp. [33]. These bacteria possess enzymes like cyanide dioxygenase, cyanidase, nitrilase, and rhodanese that allow them to transform cyanide into less toxic byproducts [34].

*Bacillus subtilis*, a ubiquitous Gram-positive bacterium, has been extensively studied for its cyanide removal abilities, making it a promising candidate for bioremediation [28,35–37]. Under alkaline conditions (pH 9–10), *B. subtilis* can efficiently degrade high cyanide concentrations (900 ppm) by expressing cyanide dihydratase enzymes [30].

Alkaline conditions favor cyanide biodegradation by reducing the volatilization of toxic HCN gas, enabling complete cyanide mineralization [34]. The high pH also provides selective advantages to alkaliphilic *B. subtilis* to outcompete other microbes. Nutrient supplementation further enhances cyanide transformation by stimulating bacterial growth [38]. Immobilized cells and genetically engineered strains of *B. subtilis* with increased cyanide dihydratase expression can be applied for efficient cyanide remediation [39].

The use of bacteria offer advantages for cyanide bioremediation, such as rapid growth, the ease of genetic modification, and an ability to withstand harsh conditions [40]. They can degrade high cyanide concentrations, operate over a range of pH levels and temperatures, and require simple nutritional inputs [30]. Applications as suspended cultures or immobilized cells enhance the stability and cyanide degradation capacity [41]. Additionally, engineered and alkaliphilic bacterial strains can be designed for optimized biodegradation under specific conditions [42].

In this study, we isolated and identified a native bacterial consortium from a sulfur mining environmental liability in Tacna, Peru. The consortium was enriched from tailing soil samples under alkaline conditions (pH 10.5) to select for bacteria adapted to the high pH, and relevant higher cyanide concentration parameters for cyanide-containing mining effluents. Batch biodegradation experiments were conducted to evaluate the cyanide removal kinetics and the efficiency of the selected bacterial strain at an alkaline pH using initial cyanide concentrations and conditions representative of real mining wastewaters.

Fourier-transform infrared (FTIR) spectroscopy was used to study the functional groups of compounds made during the biodegradation of alkaline cyanide to figure out the specific biochemical mechanisms and pathways involved.

## 2. Materials and Methods

### 2.1. Sample Collection

Soil samples were collected in high density polypropylene bags from the Tutupaca (east 0358602; north 8113940; altitude 4687 m.s.n.m.) mining environmental liabilities located in the Candarave province of Tacna, Peru. The soil samples were then homogenized and sieved to obtain 100 g of each soil sample. These were cultured in 500 mL Erlenmeyer flasks containing 100 mL of sterile distilled water, which was homogenized for 15 min to obtain the supernatant. To enrich and isolate alkaliphilic bacteria, 10 mL of the supernatant

was diluted in 90 mL of sterile nutrient broth (Merck Company, Darmstadt, Germany) and incubated at 30 °C for 24 h at 150 rpm. Then, 10 mL of this culture was inoculated into 90 mL of nutrient broth with the pH adjusted to 10.5 using sterile 0.1 N NaOH, and incubated at 30 °C for 24 h at 150 rpm. This alkaline-adapted culture was then streak-plated on nutrient agar plates (Merck Company, Darmstadt, Germany) to isolate and purify bacterial colonies capable of growing at pH 10.5 [30]. The obtained samples were labeled as TT1s, TT3s, TT7s, TT8s, TT9s, TT10s, TT11s, and TT13s, respectively.

## 2.2. Bacterial Isolation

To detect cyanide-degrading bacteria, 10 mL of the enriched culture was transferred to a 250 mL Erlenmeyer flask containing 100 mL of M9 minimal medium (g/L): Na<sub>2</sub>HPO<sub>4</sub>·7H<sub>2</sub>O (12.8); KH<sub>2</sub>PO<sub>4</sub> (3); NaCl (0.5); MgSO<sub>4</sub>·7H<sub>2</sub>O (0.5); CaCl<sub>2</sub> (0.1); 0.2% (*w/v*) sodium acetate; 0.2% (*w/v*) yeast extract; and 1% (*v/v*) mineral salt solution containing (g/L): ZnSO<sub>4</sub>·7H<sub>2</sub>O (0.05); MnCl<sub>2</sub>·4H<sub>2</sub>O (0.05); CuCl<sub>2</sub>·2H<sub>2</sub>O (0.005); Na<sub>2</sub>MoO<sub>4</sub>·2H<sub>2</sub>O (0.005); Na<sub>2</sub>B<sub>4</sub>O<sub>7</sub>·10H<sub>2</sub>O (0.002); and CoCl<sub>2</sub>·6H<sub>2</sub>O (0.0003). This was supplemented with NaCN concentrations from 100 to 1000 ppm, with the pH adjusted to 10.5 using sterile NaOH. After incubation, the viability of the isolated bacteria at each NaCN concentration was verified by streak-plating on nutrient agar plates. An alkaline pH above 10.5 was maintained to minimize the volatilization of cyanide as HCN [43–45]. Bacteria viable at cyanide levels above 1000 ppm were selected for further characterization based on their cyanide degradation potential. Gramme staining and biochemical testing were performed to verify the microscopic characteristics and taxonomy of the isolates [44].

## 2.3. Sequencing and Molecular Identification

To perform the high-throughput sequencing of bacterial genomes, high molecular weight genomic DNA was first extracted from pure cultures grown on Luria Bertani agar for 24 h at 35 °C. The InnuPREP Bacteria DNA Kit (Analytik Jena, Jena, Germany) was used for extraction, which employs enzymatic, mechanical, and chemical lysis for robust cell disruption followed by selective DNA binding to a silica spin filter for purification. DNA concentrations were then accurately quantified through fluorometry using a Qubit 4 fluorometer (Life Technologies, Carlsbad, CA, USA). For sequencing library preparation, 100 ng of genomic DNA was fragmented, end-repaired, and ligated with Illumina adapters using the Illumina DNA Prep workflow (Illumina, Granta Park, UK). Unique dual indexes from the Nextera DNA CD Indexes kit (Illumina, Granta Park, UK) were added to libraries during PCR enrichment to enable the multiplexing of samples. Finally, libraries were sequenced as 2 × 151 bp paired-end reads on the Illumina MiSeq platform using a 600-cycle reagent kit. The 16S rRNA gene sequence obtained from the potential cyanide-degrading bacterial isolate was analyzed via a comparative identity search using the BLAST (Basic Local Alignment Search Tool) against the National Center for Biotechnology Information (NCBI) database.

## 2.4. Bacterial Growth Kinetics

Bacterial growth kinetics were quantified by optical density measurements and viable plate counting. Optical density at 600 nm (OD<sub>600</sub>) was measured using a spectrophotometer (Epoch 2c, Biotek, Winooski, VT, USA) to generate high-throughput growth curves showing population expansion over time. This provided an indirect estimate of the overall cell density in the culture [45]. However, OD<sub>600</sub> does not discriminate between viable and dead cells. Therefore, viable plate counting was also carried out through dilution plating on agar and colony formation, allowing the direct quantification of colony-forming units (CFU).

## 2.5. Cyanide Biodegradation

To study the cyanide degradation capability of the selected alkaliphilic bacterial isolates, 150 mL of the M9 minimal medium was prepared and supplemented with 1000 ppm

sodium cyanide. This was inoculated with the bacteria at a density of  $10^7$ – $10^8$  cells/mL and incubated at 35 °C for 48 h with aeration at 0.2 VVM. Aliquots were taken at specific time intervals in triplicate to quantify the remaining cyanide concentration over time. The concentration of free cyanide in aliquots was determined using a titrimetric method based on Standard Methods 4500-CN-D [46]. This method relies on the reaction between silver nitrate ( $\text{AgNO}_3$ ) and cyanide ions ( $\text{CN}^-$ ) in alkaline solution to form the soluble complex silver cyanide ( $\text{Ag}(\text{CN})$ ). Specifically, a 10 mL aliquot of the sample was analyzed by adding 3 drops of potassium iodide (KI), which acts as an indicator. The sample was then titrated with a standardized  $\text{AgNO}_3$  solution. The  $\text{Ag}^+$  ions reacted with  $\text{CN}^-$  until all free cyanide had been consumed, at which point excess  $\text{Ag}^+$  reacted with the  $\text{KI}^-$  indicator to form a precipitate, marking the endpoint. The amount of  $\text{AgNO}_3$  required to reach this endpoint allows the quantification of the original free cyanide concentration. A ratio proposed by Copari et al. [12] was used to calculate the concentration, where 1 mL of  $\text{AgNO}_3$  titrant corresponds to 20 ppm of free cyanide ( $\text{CN}^-$ ) in the sample.

The cyanide degradation efficiency (DE) of the bacterial strain was calculated using the following formula [47]:

$$DE = \frac{I_c - R_c}{I_c} \cdot 100$$

where  $I_c$  is the initial concentration of cyanide (mg/L) and  $R_c$  is the residual concentration of cyanide (mg/L) after treatment.

## 2.6. Kinetic Biodegradation Models

To analyze the kinetics of cyanide biodegradation by the microorganisms, first- and second-order rate models were fit to the experimental data [48]. The first-order model assumes the reaction rate is proportional to the cyanide concentration, described mathematically as

$$\frac{dS}{dt} = k_1 S$$

where  $S$  is the cyanide concentration (mg/L),  $t$  is time (h), and  $k_1$  (1/h) is the first-order rate constant. The integration of this differential rate law gives

$$S = S_0 e^{-k_1 t}$$

where  $S_0$  is the initial cyanide concentration (mg/L).

The second-order model assumes a more complex kinetic rate law proportional to both cyanide concentration and biomass concentration:

$$\frac{dS}{dt} = -k_2 SX$$

where  $X$  is biomass concentration (mg/L) and  $k_2$  is the second-order rate constant ( $\text{mg}/(\text{mg}\cdot\text{d})$ ). This integrates to

$$k_s \ln\left(\frac{S}{S_0}\right) + S - S_0 = -k_2 t$$

where  $k_s$  is the half-saturation coefficient (mg/L).

These kinetic models were fit to experimental cyanide degradation data to estimate rate constants. The model providing the best fit, as determined by the highest correlation coefficient ( $R^2$ ), suggests the order of reaction and rate-limiting steps.

## 2.7. Analytical Methods

To study the degradation and transformation of cyanide over time, samples were collected at 0, 24, and 48 h. The samples were centrifuged at 8000 rpm for one minute to separate the cells from the supernatant. The cell-free supernatant was then analyzed using a

Fourier-transform infrared spectrometer (FTIR) equipped with an attenuated total reflection (ATR) accessory (Bruker Optics, Invenio R, Ettlingen, Germany). FTIR-ATR provides a rapid, non-destructive method to characterize molecular changes in the supernatant, letting us investigate the metabolic conversion of cyanide and identify intermediates and products formed during biodegradation. For each sample, spectra were recorded from 4000 to 400  $\text{cm}^{-1}$  at a resolution of 2  $\text{cm}^{-1}$ . Twenty scans were co-added to improve the signal-to-noise ratio, and the average spectrum was used for analysis.

### 3. Results

#### 3.1. Bacterial Isolation and Selection

Thirteen bacterial strains were isolated from soil samples collected at the Tutupaca mining site in Perú, which represents an environmental liability due to legacy contamination. Of these isolates, strains TT1s, TT3s, TT7s, TT8s, TT9s, TT10s, TT11s, and TT13s demonstrated growth viability in the presence of 100 ppm, 50 ppm, 300 ppm, 300 ppm, 600 ppm, 1000 ppm, 1000 ppm, and 600 ppm cyanide, respectively, at an alkaline pH of 10.5 (Figure 1). The isolates included Gram-negative and Gram-positive rods and cocci, with a predominance of Gram-positive, spore-forming bacilli (Table 1).

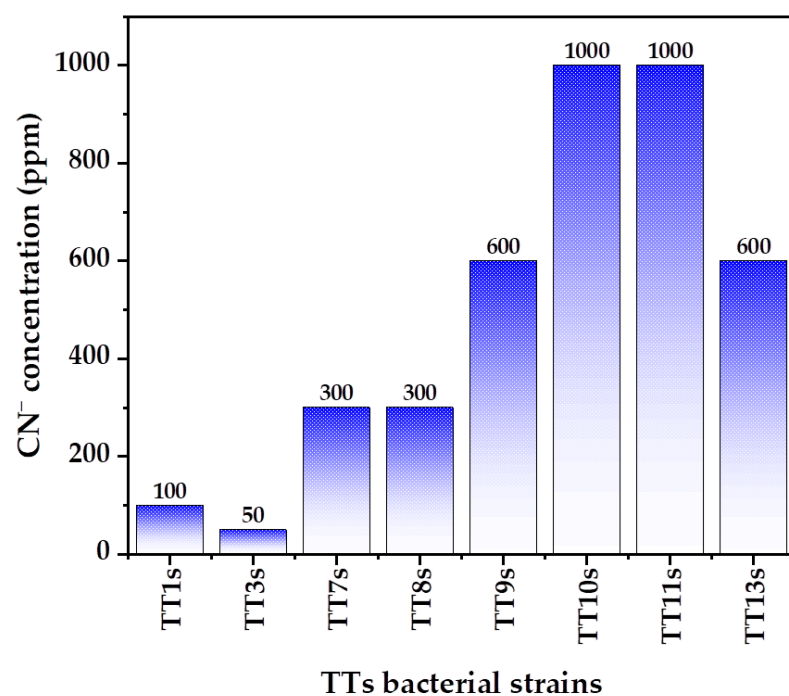


**Figure 1.** Bacterial strains surviving Tutupaca mining conditions: adapting to different cyanide Concentrations at pH 10.5 in 9 M minimal mineral medium.

**Table 1.** Morphological features of  $\text{CN}^-$ -resilient bacterial strains.

Bacterial Code	Gram Reaction	Cell Morphology	Spore Formation	Motility
TTs1	Positive	Rod chain	+	+
TTs3	Negative	Rods chain	−	−
TT7s	Negative	Rod	−	+
TT8s	Positive	Coco	−	−
TT9s	Positive	Rods	+	+
TT10s	Positive	Rods	+	+
TT11s	Positive	Rods chain	+	+
TT13s	Negative	Rods	−	+



The ability of these native isolates to tolerate high cyanide levels under alkaline conditions reflects adaptations to the selective pressure imposed by legacy mining pollution at the site [49]. The predominance of *Bacillus* species is consistent with prior research showing their competence in alkaline cyanide biodegradation [50–52]. The cyanide tolerance of these isolates suggests they likely possess enzymatic pathways for cyanide transformation as a detoxification mechanism [53].

The various biochemical assays were performed for the selection strain TT10s, due to its capacity for viable survival up to 1000 ppm and its quick growth. The results coincided with the genus *Bacillus* (Table 2) [54]. Specifically, TT10s was found to be catalase and oxidase positive, methyl red negative, Voges–Proskauer positive, urease negative, able to use citrate, and capable of nitrate reduction. The strain could utilize glucose, mannitol, lactose, D-xylose, and sucrose as sole carbon sources, but not maltose [55]. No indole production was detected. Taken together, these biochemical characteristics are consistent with *Bacillus* spp. [56], supporting the identification of TT10s as a novel *Bacillus* strain with potential industrial applications due to its high tolerance to toxins.

**Table 2.** Biochemical analysis of CN<sup>−</sup>-resilient bacterial strain TT10s.

Bacterial	Catalase	Oxidase	MR	VP	Citrate	Urease	Nitrate	Glucose	Maltose	Mannitol	Lactose/N <sub>2</sub>	D-Xylose	Sucrose/Indole
TT10s	+	+	−	+	+	−	+	+	−	+	+	+	+

### 3.2. Molecular Identification

The 16S rRNA gene sequence of the isolated strain TT10s was elucidated using the BLAST alignment tool and compared to nucleotide sequences in the NCBI GenBank database. The nearly complete 1538 bp sequence exhibited 100% similarity with three *Bacillus* species: *Bacillus rugosus* (sequence IDs: MT554518.1, NR\_181236.1, CP096590.1), *Bacillus subtilis* (sequence IDs: CP\_025941.1, CP\_018172.1, KR967391.1, OL636042.1), and *Bacillus stercoris* (sequence IDs: CP126678.1, CP124601.1). A phylogenetic analysis using the maximum likelihood algorithm positioned TT10s within the *B. subtilis* clade with strong bootstrap support. Taken together, this molecular identification aligned with the observed morphological properties of TT10s, including Gram-positive rods that form endospores and biochemical characteristics such as catalase and urease activity and the ability to utilize D-xylose and citrate (Tables 1 and 2). Based on an integrative taxonomic analysis of phenotypic, microscopic, and 16S rRNA sequence data, the isolated bacterial strain TT10s can be definitively classified as belonging to *Bacillus subtilis* because this species is urease positive and D-xylose negative, in contrast to *Bacillus stercoris* and *Bacillus rugosus*, which are negative and positive, respectively [57–59]. The gene sequence was deposited in the GenBank nucleotide archive under accession number OR505001 for reference.

### 3.3. Growth Kinetics

The relation between the OD optical density and the natural logarithm of the bacterial growth in CFU/mL of the TT10s bacterium was determined by means of a linear adjustment of its growth curve (Figure 2), determining an R<sup>2</sup> of 0.94 for the TT10s bacterium. Although this method may interfere with the results, due to the detection of non-cellular solids in the samples, it is advantageous due to its speed and automation [60]. For this reason, this calibration curve was made with replicas to estimate the bacterial growth of live cells in the biodegradation process of the TT10s bacterium.

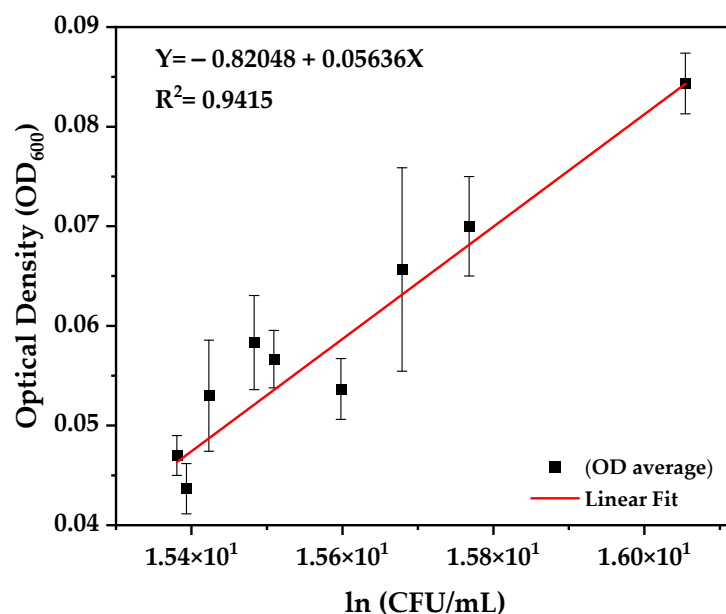


**Figure 2.** Linear fitting of bacterial growth for bacterial strain TT10s in OD600 (Abs) and Ln plate count (CFU/mL).

### 3.4. Cyanide Biodegradation

The biodegradation study of free cyanide was carried out via sampling every 6 h for the bacterial strain TT10s, as it was the strain with the greatest viability capacity at concentrations up to 1000 ppm in the M9 mineral medium at a pH of 10.5, temperature of 35 °C, and 0.2 vvm. This TT10s bacterial strain presented a degradation of 1000 ppm cyanide in less than 48 h (Table 3), with a degradation efficiency of up to 100% at 48 h and a maximum bacterial growth of up to  $1.583 \times 10^1$  (ln CFU/mL) at 18 h (Figure 3).

**Table 3.** Cyanide degradation efficiency (%) and Ln bacterial growth (CFU/mL) for TT10s bacteria.

Time (h)	CN <sup>-</sup> Degradation Efficiency (%)	SD	Plate Count Ln (CFU/mL)	SD
0	0.00	0.00	15.70	0.00
6	20.67	1.53	15.55	0.04
12	41.07	1.10	15.64	0.09
18	63.60	0.40	15.83	0.06
24	86.87	2.58	15.58	0.03
30	90.80	2.23	15.51	0.05
36	94.53	0.46	15.38	0.05
42	99.63	0.06	15.26	0.01
48	100.00	0.00	15.18	0.01

Bacterial growth was measured with ln CFU/mL, and peaked at  $1.583 \times 10^1$  at 18 h before decreasing. This growth curve is typical for batch culture, with exponential growth followed by stationary and death phases [30].

The rapid and complete cyanide biodegradation by TT10s demonstrates its potential for industrial applications in treating cyanide waste streams compared to other bacterial strains, according to Table 4. The alkaline conditions prevented volatile HCN formation, enhancing process safety [61].

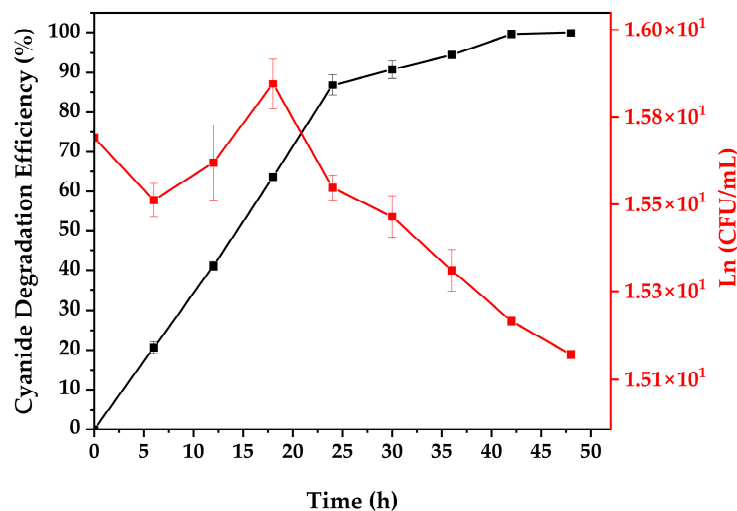


**Figure 3.** Cyanide degradation efficiency% in relation to time and *Bacillus subtilis* bacterial growth within 48 h.

**Table 4.** Cyanide biodegradation performances of various bacteria.

Bacterium	Experimental Conditions	Cyanide Degradation	Reference
<i>Bacillus subtilis</i>	48 h, pH 10.5, 30 °C, 1000 mg/L initial cyanide	100%	Present work
<i>Pseudomonas putida</i>	24 h, pH 9, 30 °C, 100 mg/L initial cyanide	90%	[26]
<i>Pseudomonas fluorescens</i>	48 h, pH 7, 30 °C, 50 mg/L initial cyanide	80%	[62]
<i>Bacillus</i> sp.	96 h, pH 9.88, 33.6 °C, 500 mg/L initial cyanide	99%	[51]
<i>Klebsiella pneumoniae</i>	72 h, pH 7, 25 °C, 25 mg/L initial cyanide	87%	[63]
<i>Bacillus cereus</i>	48 h, pH 7, 37 °C, 100 mg/L initial cyanide	95.87%	[64]

The isolated *Bacillus subtilis* strain TT10s demonstrated exceptionally rapid and complete cyanide degradation under alkaline conditions compared to the other bacteria studied. As shown in Table 4, TT10s achieved a 100% removal of a high initial cyanide concentration of 1000 mg/L within 48 h at pH 10.5, significantly outperforming various *Pseudomonas*, *Klebsiella*, and other *Bacillus* species strains, which required longer times or achieved only 60–90% removal at lower cyanide loadings and pH. The kinetic analysis indicates the specialized enzymatic pathways of TT10s enabled uniquely efficient cyanide metabolism rates even at elevated pH where volatile toxic HCN production is minimized. The rapid total degradation by TT10s shows great promise for the industrial bioremediation of alkaline cyanide effluents compared to currently studied bacteria.

### 3.5. Kinetic Models

Kinetic modeling was performed to elucidate the rate law and mechanisms governing cyanide biodegradation by *Bacillus subtilis*. Determining the most appropriate model that accurately depicts the kinetics is crucial for mechanistic insight. The experimental data strongly fit a second-order rate model ( $k_2 = 0.08649 \text{ mg}/(\text{mg}\cdot\text{h})$ ,  $R^2 = 0.96622$ ) better than a first-order model ( $k_1 = 0.11394 \text{ 1/h}$ ,  $R^2 = 0.8514$ ), as shown in Figure 4. Several factors justify selecting the second-order kinetics, but principally they exhibited a statistically stronger empirical fit with a higher coefficient of determination ( $R^2$ ), agreeing with the literature in showing second-order dependence on the rate-limiting cyanide dihydratase enzyme [26,34,65]. Cyanide dihydratase catalyzes the conversion of cyanide to ammonia and formate via Michaelis–Menten kinetics as an inducible enzyme requiring cyanide as a substrate [65–68]. The higher coefficient of determination ( $R^2$ ) and lower second-order rate constant ( $k_2$ ) compared to the first-order rate constant ( $k_1$ ) indicate that the second-order model more accurately reflects the enzymatic rate-limiting mechanism. Additional evidence



comes from the observed lag phase, of up to 12 h, attributed to enzyme induction [69], an exponential phase from 12 to 30 h as enzyme levels increase, and a plateau after 30 h, indicating saturation kinetics.

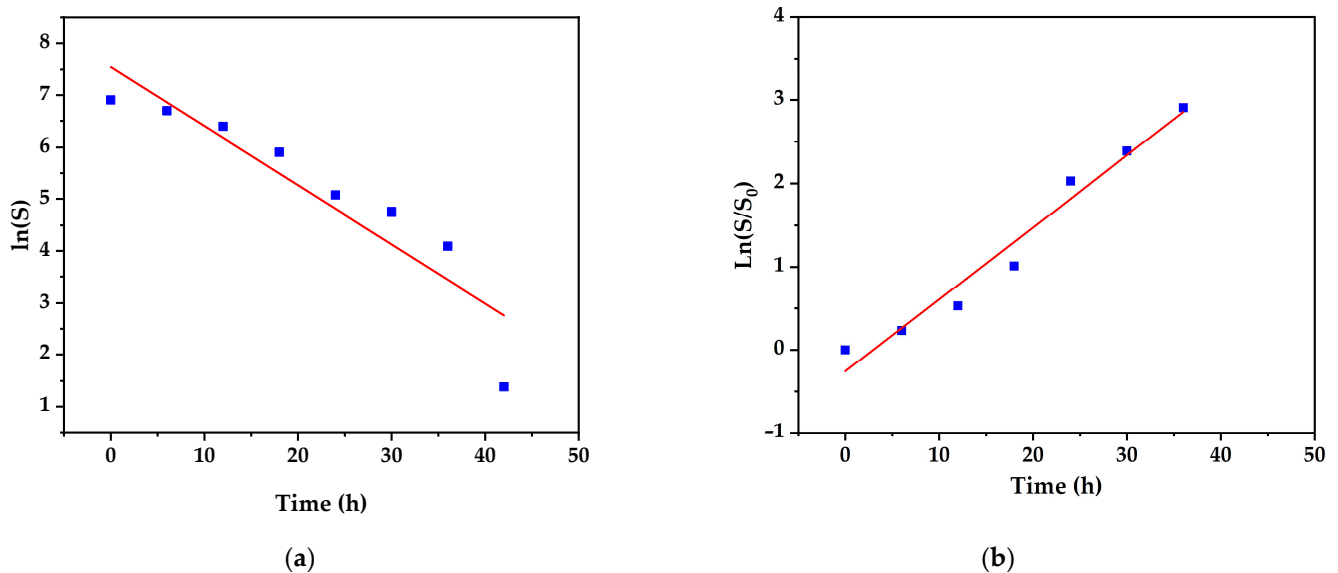


**Figure 4.** Kinetic model of the cyanide degradation; (a) first order and (b) second order fitting plots.

### 3.6. FTIR Spectroscopy Analysis

The FTIR spectra shown in Figure 5 indicate several key changes occurring during the 48 h period that align with cyanide being degraded into ammonia and formate by the *Bacillus subtilis* strain via the cyanide dihydratase enzymatic pathway.

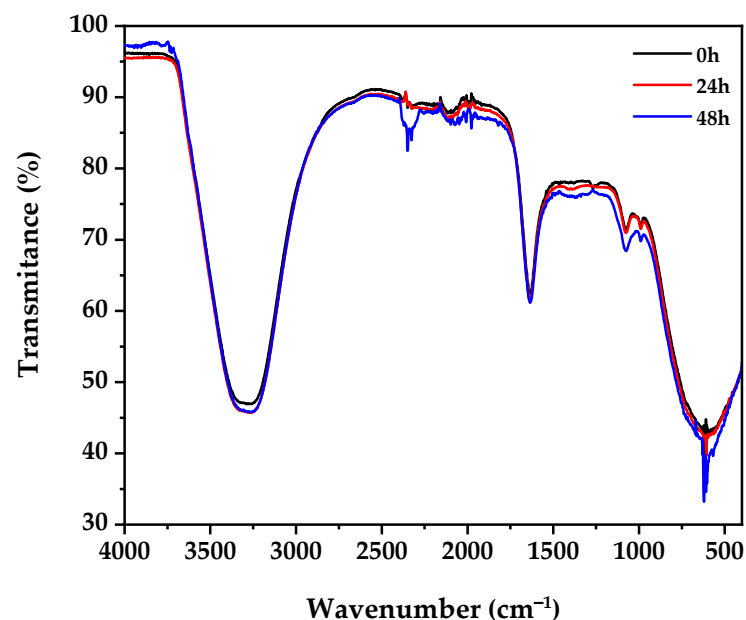


**Figure 5.** FTIR spectra of supernatant samples taken at initial time, 24, and 48 h.

Specifically, the peaks at 2120–2260  $\text{cm}^{-1}$  corresponding to  $\text{C}\equiv\text{N}$  stretching vibrations [70] decreased over time. This directly reflects cyanide levels being metabolized by the bacteria. Concurrently, a broad peak around 3300  $\text{cm}^{-1}$  is associated with OH and NH vibrations and this increased as the end product ammonia built up [71]. A third notable change is the growth of the peak at 1550–1750  $\text{cm}^{-1}$  related to  $\text{C}=\text{O}$  vibrations from generated formate [72].

Taken together, the kinetic disappearance of cyanide bands and the emergence of ammonia and formate features provide strong spectroscopic evidence corroborating the proposed cyanide dihydratase mechanism. The second-order rate behavior reflects how this inducible enzymatic process controls the biodegradation pace.

#### 4. Discussion

Cyanide is a highly toxic compound to living organisms that is used in various economic activities, mainly related to mining [73,74]. These mineral extraction activities generate wastes contaminated with heavy metals or toxic substances like CN that disperse into the environment [13,75]. This study isolated eight bacterial strains from a soil sample with sulfur mining residues that could tolerate 50–1000 ppm CN under alkaline conditions (Figure 1). Strain TT10s was identified as *Bacillus subtilis* and chosen for further study due to its exceptional ability to withstand and degrade high cyanide concentrations under alkaline conditions compared to prior *B. subtilis* strains and its rapid growth rate.

The identification of this species within a very diverse genus was accomplished through its phenotypic characteristics in relation to nutritional requirements, growth conditions (Tables 1 and 2), and DNA composition [76]. The 16S rRNA gene sequence confirms TT10s as a *B. subtilis* strain, sharing 100% nucleotide similarity. However, TT10s possesses unique functional capabilities, enabling rapid and thorough cyanide mineralization under alkaline conditions relevant for mining effluents.

Previous studies reported a 92–500 ppm cyanide tolerance of *B. subtilis* isolates [28,77], and TT10s survived up to 1000 ppm cyanide at pH 10.5. Additionally, TT10s achieved a complete degradation of 1000 ppm cyanide in just 48 h (Figure 3), far exceeding the 60–72 h timeframes for 500 ppm removal reported for other strains [28]. Other *Bacillus* species degraded lower CN concentrations, like *B. pumilus* up to 500 ppm [73]. Many bacterial genera like *Pseudomonas*, *Rhodococcus*, *Klebsiella*, and *Bacillus* can biodegrade CN, with specific strains listed in Table 4. These bacteria likely use metabolic pathways to completely degrade or transform CN into less harmful products [78,79], utilizing CN as nitrogen and carbon sources [34,80].

Degradation kinetics revealed a second order rate ( $k_2 = 0.08649$  mg/(mg·h),  $R^2 = 0.96622$ ) (Figure 4). The second-order rate law integrates both reactant (cyanide) and biocatalyst (bacterial cells) concentrations, consistent with the reaction being mediated by inducible bacterial enzymes that increase in amount with microbial growth [81]. Specifically, the cyanide dihydratase enzyme was synthesized by *Bacillus subtilis* in response to cyanide, which served as both inducer and substrate. Thus, the reaction rate depended on the concentrations of both cyanide and induced cyanide dihydratase, aligning with the second-order model [28].

Based on FTIR analysis (Figure 5), the hydrolytic pathway in *B. subtilis* produced ammonia and formate, characteristic of enzymatic CN triple bond cleavage mediated by water molecules [34,82]. *B. subtilis* converted this pollutant into less toxic substances [83]. Similar traits occurred in *B. safensis*, *B. cereus*, and *B. pumilus*, degrading CN enzymatically via cyanide dihydratase into ammonia and formate, with active enzymes up to pH 9 [22,84–86]. Some *Bacillus* species do not require cofactors for CN degradation [85,86]. The ability of *B. subtilis* to degrade CN without extra carbon sources at pH up to 10.5 shows its degradation enzyme functions under high pH levels, CN concentration, and without other nutrients.

Unlike other bacteria, that require additional nutrients to be more efficient in the biodegradation process [87,88], this bacterium performed the biodegradation process at a pH adjusted to 10.5 so that the CN remained dissolved in the medium rather than transforming into HCN [89]. This parameter provides an advantage and is one of the most important factors during biodegradation treatment [30,90]. Because *Bacillus* species are key producers of extracellular proteases, with potential applications to function and maintain stability under extreme alkaline conditions between pH 9–12 through sophisticated intracellular proton transport mechanisms for their growth [80], these proteases are induced

for production by medium conditions like pH, temperature, and aeration, and strongly influenced by the available carbon and nitrogen components [81].

Using bacteria like *B. subtilis* for biodegradation with advantageous traits can enable applications in contaminated environments in an eco-friendly manner with minimal toxic byproducts [83]. Optimal conditions like temperature, pH, aeration, and nutrient availability should be ensured for efficient CN removal [74,91]. Bacterial biodegradation, with 85–98% efficiency, is more economical and eco-friendly than physical/chemical methods, generating minimal waste [73]. The highly efficient cyanide degradation capacity of the *Bacillus subtilis* strain under alkaline conditions holds significance for mitigating cyanide pollution from diverse industries like mining, textiles, metal finishing, and other industries that generate alkaline effluents [26]. Due to this, conventional remediation methods are hampered by variations in conditions, high costs, and hazardous byproducts [3].

At present, research efforts are crucial to fine-tune the biodegradation process of *B. subtilis* and elucidate its genetic underpinnings concerning cyanide degradation. The harnessing of *B. subtilis* holds immense potential for effective cyanide remediation in both aquatic and terrestrial ecosystems affected by contamination. This versatile bacterium presents an opportunity for the low-cost, environmentally friendly cleanup of cyanide-contaminated waters and soils, particularly at lower pH ranges. The progress made in this research sets a pivotal foundation for the development of a sustainable and eco-friendly biotechnological solution, addressing the pressing challenges posed by cyanide pollution.

## 5. Conclusions

This study isolated a novel *Bacillus subtilis* strain designated TT10s from mining environmental liabilities that demonstrated efficient cyanide biodegradation capacity.

The analysis of the 16S rRNA gene sequence established the phylogenetic classification of TT10s as *Bacillus subtilis*. This novel isolate displayed rapid adaptation and cyanide degradation under alkaline conditions with no need for extra carbon source conditions.

The biodegradation experiments showed that *Bacillus subtilis* demonstrated exceptional cyanide degradation capacity under alkaline conditions of pH 10.5, achieving the 100% removal of an initial cyanide concentration of 1000 ppm in less than 48 h.

Kinetic experiments revealed that the cyanide degradation followed second-order rate kinetics ( $k_2 = 0.08649 \text{ mg}/(\text{mg}\cdot\text{h})$  and  $R^2 = 0.96622$ ), with dependence on both cyanide concentration and bacterial density.

The quantitative kinetics aligned with an enzymatic mechanism governed by cyanide dihydratase, which converts cyanide into ammonia and formate. FTIR analysis provided additional spectroscopic evidence supporting this enzymatic reaction. The kinetic and FTIR data implicate cyanide dihydratase as the rate-controlling enzyme in alkaline cyanide biodegradation by TT10s.

**Author Contributions:** Conceptualization C.J.C.Q. and G.d.L.F.Q.; methodology, G.d.L.F.Q.; software, G.d.L.F.Q. and E.J.S.S.; validation, C.J.C.Q., G.d.L.F.Q. and E.J.S.S.; formal analysis, C.J.C.Q.; investigation, C.J.C.Q. and G.d.L.F.Q.; resources, C.J.C.Q.; data curation, G.d.L.F.Q.; writing—original draft preparation, C.J.C.Q., G.d.L.F.Q. and E.J.S.S.; writing—review and editing, C.J.C.Q., G.d.L.F.Q., E.J.S.S., M.C.M. and G.J.M.C.; visualization, G.d.L.F.Q.; supervision, C.J.C.Q.; project administration, G.d.L.F.Q.; funding acquisition, C.J.C.Q. All authors have read and agreed to the published version of the manuscript.

**Funding:** This research and APC were funded by the Universidad Nacional Jorge Basadre Grohmann through “Fondos del canon sobrecanon y regalías mineras”, approved by Rectoral Resolution N° 4723-2015-UN/JBG, with the project “Análisis genómico de microorganismos degradadores de cianuro para la remediación, en fase de biorreactor de pasivos ambientales mineros de la región de Tacna”.

**Data Availability Statement:** The data presented in this study are available within this article.

**Acknowledgments:** We are grateful to the project “Determination of the optical fingerprints of solid, liquid and organic materials using visible and infrared spectroscopy”, of the Universidad Nacional

Jorge Basadre Grohmann, approved by rectoral resolutions N° 5854-2019-UN/JBG, for their support in the FTIR analysis.

**Conflicts of Interest:** The authors declare no conflict of interest.

## References

- Wang, Z.-S.; Cho, Y.-C.; Lin, Y.-P. Removal of Cyanide from Electroplating Wastewater by Persulfate Oxidation Process. 2023. Available online: <https://ssrn.com/abstract=4427783> (accessed on 28 September 2023).
- Eisler, R.; Wiemeyer, S.N. Cyanide hazards to plants and animals from gold mining and related water issues. *Rev. Environ. Contam. Toxicol.* **2004**, *183*, 21–54. [[CrossRef](#)] [[PubMed](#)]
- Martínková, L.; Bojarová, P.; Sedova, A.; Kfen, V. Recent trends in the treatment of cyanide-containing effluents: Comparison of different approaches. *Crit. Rev. Environ. Sci. Technol.* **2023**, *53*, 416–434. [[CrossRef](#)]
- Cacciuttolo, C.; Cano, D. Environmental Impact Assessment of Mine Tailings Spill Considering Metallurgical Processes of Gold and Copper Mining: Case Studies in the Andean Countries of Chile and Peru. *Water* **2022**, *14*, 3057. [[CrossRef](#)]
- Matlock, M.M.; Howerton, B.S.; van Aelstyn, M.A.; Nordstrom, F.L.; Atwood, D.A. Advanced mercury removal from gold leachate solutions prior to gold and silver extraction: A field study from an active gold mine in Peru. *Environ. Sci. Technol.* **2002**, *36*, 1636–1639. [[CrossRef](#)]
- Isla, A. The Guardians of Conga Lagoons: Defending Land Water and Freedom in Peru. *Can. Woman Stud./Les Cah. De La Femme* **2015**, *30*, 25–40.
- Presidencia del Consejo de Ministros de Perú. Decreto Supremo que Declara el Estado de Emergencia en los Distritos de Cocachacra, Dean Valdivia y Punta de Bombón de la Provincia de Islay, del Departamento de Arequipa, por Peligro Inminente Ante Contaminación Hídrica; Perú, 2021 (N° 106-2021-PCM). Available online: <https://busquedas.elperuano.pe/dispositivo/NL/1957547-2> (accessed on 26 September 2023).
- Bebbington, A.; Williams, M. Water and Mining Conflicts in Peru. *Mt. Res. Dev.* **2008**, *28*, 190–195. [[CrossRef](#)]
- Salem, J.; Amonkar, Y.; Maennling, N.; Lall, U.; Bonnafous, L.; Thakkar, K. An analysis of Peru: Is water driving mining conflicts? *Resour. Policy* **2021**, *74*, 101270. [[CrossRef](#)]
- Ministerio del Ambiente. Modifican los Estándares Nacionales de Calidad Ambiental Para Agua y Establecen Disposiciones Complementarias Para su Aplicación; Diario el Peruano, 2015 (N° 015-2015-MINAM). Available online: <https://www.minam.gob.pe/wp-content/uploads/2015/12/Decreto-Supremo-N%C2%B0-015-2015-MINAM.pdf> (accessed on 28 September 2023).
- Marshall, B.G.; Veiga, M.M.; Da Silva, H.A.M.; Guimarães, J.R.D. Cyanide Contamination of the Puyango-Tumbes River Caused by Artisanal Gold Mining in Portovelo-Zaruma, Ecuador. *Curr. Environ. Health Rep.* **2020**, *7*, 303–310. [[CrossRef](#)]
- Copari Mamani, A.B.; Carpio Mamani, M.; Cáceda Quiroz, C.J. Optimización de factores fisicoquímicos en la biodegradación de cianuro por *Klebsiella* sp.ART1, en biorreactor aireado. *Cienc. Desarro.* **2020**, *26*, 20–31. [[CrossRef](#)]
- Quiroz, C.J.C.; Choque, G.J.M.; Mamani, M.C.; Quispe, G.D.L.F. Evaluation of the content of metals and contamination indices generated by environmental liabilities, in Tacna, Peru. *Res. Sq.* **2022**. [[CrossRef](#)]
- Swenson, J.J.; Carter, C.E.; Domec, J.-C.; Delgado, C.I. Gold mining in the Peruvian Amazon: Global prices, deforestation, and mercury imports. *PLoS ONE* **2011**, *6*, e18875. [[CrossRef](#)]
- Veiga, M.M.; Angeloci, G.; Hitch, M.; Colon Velasquez-Lopez, P. Processing centres in artisanal gold mining. *J. Clean. Prod.* **2014**, *64*, 535–544. [[CrossRef](#)]
- Mayorca Clemente, S. *Reducción de Cianuro Del Agua Industrial Contaminada Mediante Biopelícula Microbiana, Chala—Arequipa 2018*; Universidad César Vallejo: Lima, Peru, 2018.
- Vuono, D.C.; Vanneste, J.; Figueroa, L.A.; Hammer, V.; Aguilar-Huaylla, F.N.; Malone, A.; Smith, N.M.; Garcia-Chevesich, P.A.; Bolaños-Sosa, H.G.; Alejo-Zapata, F.D.; et al. Photocatalytic Advanced Oxidation Processes for Neutralizing Free Cyanide in Gold Processing Effluents in Arequipa, Southern Peru. *Sustainability* **2021**, *13*, 9873. [[CrossRef](#)]
- Asner, G.P.; Tupayachi, R. Accelerated losses of protected forests from gold mining in the Peruvian Amazon. *Environ. Res. Lett.* **2016**, *12*, 94004. [[CrossRef](#)]
- Downey, J.; Basi, K.; DeFreytas, M.; Rockwood, G.; Chronic cyanide exposure. *Case Studies and Animal Models in Toxicology of Cyanides and Cyanogens: Experimental, Applied and Clinical Aspects*, 1st ed.; Hall, A.H., Isom, G.E., Rockwood, G.A., Eds.; John Wiley & Sons: Chichester, UK, 2015; pp. 21–40. ISBN 978-1119978534.
- Shifrin, N.S.; Beck, B.D.; Gauthier, T.D.; Chapnick, S.D.; Goodman, G. Chemistry, toxicology, and human health risk of cyanide compounds in soils at former manufactured gas plant sites. *Regul. Toxicol. Pharmacol.* **1996**, *23*, 106–116. [[CrossRef](#)]
- Kuyucak, N.; Akcil, A. Cyanide and removal options from effluents in gold mining and metallurgical processes. *Miner. Eng.* **2013**, *50–51*, 13–29. [[CrossRef](#)]
- Sharma, M.; Akhter, Y.; Chatterjee, S. A review on remediation of cyanide containing industrial wastes using biological systems with special reference to enzymatic degradation. *World J. Microbiol. Biotechnol.* **2019**, *35*, 70. [[CrossRef](#)]
- Akcil, A. Destruction of cyanide in gold mill effluents: Biological versus chemical treatments. *Biotechnol. Adv.* **2003**, *21*, 501–511. [[CrossRef](#)]
- Luque-Almagro, V.M.; Moreno-Vivián, C.; Roldán, M.D. Biodegradation of cyanide wastes from mining and jewellery industries. *Curr. Opin. Biotechnol.* **2016**, *38*, 9–13. [[CrossRef](#)]

25. Kunz, D.A.; Wang, C.S.; Chen, J.L. Alternative routes of enzymic cyanide metabolism in *Pseudomonas fluorescens* NCIMB 11764. *Microbiology* **1994**, *140 Pt 7*, 1705–1712. [[CrossRef](#)]
26. Dash, R.R.; Gaur, A.; Balomajumder, C. Cyanide in industrial wastewaters and its removal: A review on biotreatment. *J. Hazard. Mater.* **2009**, *163*, 1–11. [[CrossRef](#)] [[PubMed](#)]
27. Castric, P.A.; Strobel, G.A. Cyanide Metabolism by *Bacillus megaterium*. *J. Biol. Chem.* **1969**, *244*, 4089–4094. [[CrossRef](#)]
28. Rosario, C.G.A.; Vallenás-Arévalo, A.T.; Arévalo, S.J.; Espinosa, D.C.R.; Tenório, J.A.S. Biodegradation of cyanide using a *Bacillus subtilis* strain isolated from artisanal gold mining tailings. *Braz. J. Chem. Eng.* **2023**, *40*, 129–136. [[CrossRef](#)]
29. Meyers, P.R.; Gokool, P.; Rawlings, D.E.; Woods, D.R. An efficient cyanide-degrading *Bacillus pumilus* strain. *J. Gen. Microbiol.* **1991**, *137*, 1397–1400. [[CrossRef](#)] [[PubMed](#)]
30. Alvillo-Rivera, A.; Garrido-Hoyos, S.; Buitrón, G.; Thangarasu-Sarasvathi, P.; Rosano-Ortega, G. Biological treatment for the degradation of cyanide: A review. *J. Mater. Res. Technol.* **2021**, *12*, 1418–1433. [[CrossRef](#)]
31. Liu, J.K.; Liu, C.H.; Lin, C.S. The role of nitrogenase in a cyanide-degrading *Klebsiella oxytoca* strain. *Proc. Natl. Sci. Counc. Repub. China B* **1997**, *21*, 37–42. [[PubMed](#)]
32. Adjei, M.D.; Ohta, Y. Isolation and characterization of a cyanide-utilizing *Burkholderia cepacia* strain. *World J. Microbiol. Biotechnol.* **1999**, *15*, 699–704. [[CrossRef](#)]
33. Nallapan Maniyam, M.; Sjahrir, F.; Ibrahim, A.L.; Cass, A.E.G. Biodegradation of cyanide by acetonitrile-induced cells of *Rhodococcus* sp. UKMP-5M. *J. Gen. Appl. Microbiol.* **2013**, *59*, 393–404. [[CrossRef](#)]
34. Ebbs, S. Biological degradation of cyanide compounds. *Curr. Opin. Biotechnol.* **2004**, *15*, 231–236. [[CrossRef](#)]
35. Nwokoro, O.; Dibia, M.E.U. Degradation of soil cyanide by single and mixed cultures of *Pseudomonas stutzeri* and *Bacillus subtilis*. *Arh. Hig. Rada Toksikol.* **2014**, *65*, 113–119. [[CrossRef](#)]
36. Niu, H.; Volesky, B. Characteristics of gold biosorption from cyanide solution. *J. Chem. Technol. Biotechnol.* **1999**, *74*, 778–784. [[CrossRef](#)]
37. Knowles, C.J. Cyanide utilization and degradation by microorganisms. *Ciba Found. Symp.* **1988**, *140*, 3–15. [[CrossRef](#)] [[PubMed](#)]
38. Patil, Y.; Paknikar, K. Development of a process for biodegradation of metal cyanides from waste waters. *Process Biochem.* **2000**, *35*, 1139–1151. [[CrossRef](#)]
39. Obed Ntwampe, S.K. Biodegradation of Free Cyanide Using *Bacillus* Sp. Consortium Dominated by *Bacillus Safensis*, *Lichenformis* and *Tequilensis* Strains: A Bioprocess Supported Solely with Whey. *J. Bioremediation Biodegrad.* **2014**, *5*. [[CrossRef](#)]
40. Akcil, A.; Karahan, A.; Ciftci, H.; Sagdic, O. Biological treatment of cyanide by natural isolated bacteria (*Pseudomonas* sp.). *Miner. Eng.* **2003**, *16*, 643–649. [[CrossRef](#)]
41. Nallapan Maniyam, M.; Sjahrir, F.; Ibrahim, A.L.; Cass, A.E.G. Cyanide degradation by immobilized cells of *Rhodococcus* UKMP-5M. *Biologia* **2012**, *67*, 837–844. [[CrossRef](#)]
42. Ozkan, M.; Desai, S.G.; Zhang, Y.; Stevenson, D.M.; Beane, J.; White, E.A.; Guerinot, M.L.; Lynd, L.R. Characterization of 13 newly isolated strains of anaerobic, cellulolytic, thermophilic bacteria. *J. Ind. Microbiol. Biotechnol.* **2001**, *27*, 275–280. [[CrossRef](#)]
43. Mirzadeh, S.; Yaghmaei, S.; Ghobadi Nejad, Z. Biodegradation of cyanide by a new isolated strain under alkaline conditions and optimization by response surface methodology (RSM). *J. Environ. Health Sci. Eng.* **2014**, *12*, 85. [[CrossRef](#)]
44. Kumar, V.; Kumar, V.; Bhalla, T.C. Statistical Enhancement of Cyanide Degradation Using Microbial Consortium. *J. Microb. Biochem. Technol.* **2015**, *7*, 6. [[CrossRef](#)]
45. Huertas, M.J.; Sáez, L.P.; Roldán, M.D.; Luque-Almagro, V.M.; Martínez-Luque, M.; Blasco, R.; Castillo, F.; Moreno-Vivián, C.; García-García, I. Alkaline cyanide degradation by *Pseudomonas pseudoalcaligenes* CECT5344 in a batch reactor. Influence of pH. *J. Hazard. Mater.* **2010**, *179*, 72–78. [[CrossRef](#)]
46. Rice, E.W.; Baird, R.B.; Eaton, A.D. *Standard Methods For the Examination of Water and Wastewater*; American Public Health Association: Washington, DC, USA, 2017; ISBN 978-0-87553-299-8.
47. Kandasamy, S.; Dananjeyan, B.; Krishnamurthy, K.; Benckiser, G. Aerobic cyanide degradation by bacterial isolates from cassava factory wastewater. *Braz. J. Microbiol.* **2015**, *46*, 659–666. [[CrossRef](#)] [[PubMed](#)]
48. Alvarado-López, M.J.; Garrido-Hoyos, S.E.; Raynal-Gutiérrez, M.E.; El-Kassis, E.G.; Luque-Almagro, V.M.; Rosano-Ortega, G. Cyanide Biodegradation by a Native Bacterial Consortium and Its Potential for Goldmine Tailing Biotreatment. *Water* **2023**, *15*, 1595. [[CrossRef](#)]
49. Ibrahim, K.K.; Syed, M.A.; Shukor, M.Y.; Ahmad, S.A. Biological Remediation of Cyanide: A Review. *Biotropia* **2016**, *22*, 151–163. [[CrossRef](#)]
50. Mekuto, L.; Alegbeleye, O.O.; Ntwampe, S.K.O.; Ngongang, M.M.; Mudumbi, J.B.; Akinpelu, E.A. Co-metabolism of thiocyanate and free cyanide by *Exiguobacterium acetylicum* and *Bacillus marisflavi* under alkaline conditions. *3 Biotech* **2016**, *6*, 173. [[CrossRef](#)]
51. Mekuto, L.; Ntwampe, S.K.O.; Jackson, V.A. Biodegradation of free cyanide and subsequent utilisation of biodegradation by-products by *Bacillus* consortia: Optimisation using response surface methodology. *Environ. Sci. Pollut. Res. Int.* **2015**, *22*, 10434–10443. [[CrossRef](#)]
52. Wu, C.-F.; Xu, X.-M.; Zhu, Q.; Deng, M.-C.; Feng, L.; Peng, J.; Yuan, J.-P.; Wang, J.-H. An effective method for the detoxification of cyanide-rich wastewater by *Bacillus* sp. CN-22. *Appl. Microbiol. Biotechnol.* **2014**, *98*, 3801–3807. [[CrossRef](#)]
53. Dubey, S.K.; Holmes, D.S. Biological cyanide destruction mediated by microorganisms. *World J. Microbiol. Biotechnol.* **1995**, *11*, 257–265. [[CrossRef](#)]



54. Slepecky, R.A.; Hemphill, H.E. The Genus *Bacillus*—Nonmedical. In *The Prokaryotes*; Dworkin, M., Falkow, S., Rosenberg, E., Schleifer, K.-H., Stackebrandt, E., Eds.; Springer: New York, NY, USA, 2006; pp. 530–562. ISBN 978-0-387-25494-4.
55. Stülke, J.; Hillen, W. Regulation of carbon catabolism in *Bacillus* species. *Annu. Rev. Microbiol.* **2000**, *54*, 849–880. [[CrossRef](#)]
56. Berkeley, R.; Logan, N.A.; Shute, L.A.; Capey, A.G. *12 Identification of Bacillus Species*; Elsevier: Amsterdam, The Netherlands, 1984; pp. 291–328. ISBN 9780125215169.
57. Bhattacharya, D.; de Los Santos Villalobos, S.; Ruiz, V.V.; Selvin, J.; Mukherjee, J. *Bacillus rugosus* sp. nov. producer of a diketopiperazine antimicrobial, isolated from marine sponge *Spongia officinalis* L. *Antonie Van Leeuwenhoek* **2020**, *113*, 1675–1687. [[CrossRef](#)]
58. Gatson, J.W.; Benz, B.F.; Chandrasekaran, C.; Satomi, M.; Venkateswaran, K.; Hart, M.E. *Bacillus tequilensis* sp. nov., isolated from a 2000-year-old Mexican shaft-tomb, is closely related to *Bacillus subtilis*. *Int. J. Syst. Evol. Microbiol.* **2006**, *56*, 1475–1484. [[CrossRef](#)]
59. Dunlap, C.A.; Bowman, M.J.; Zeigler, D.R. Promotion of *Bacillus subtilis* subsp. *inaquosorum*, *Bacillus subtilis* subsp. *spizizenii* and *Bacillus subtilis* subsp. *stercoris* to species status. *Antonie Van Leeuwenhoek* **2020**, *113*, 1–12. [[CrossRef](#)] [[PubMed](#)]
60. Muloiwa, M.; Nyende-Byakika, S.; Dinka, M. Comparison of unstructured kinetic bacterial growth models. *S. Afr. J. Chem. Eng.* **2020**, *33*, 141–150. [[CrossRef](#)]
61. Malone, S.L.; Pearce, L.L.; Peterson, J. Environmental toxicology of cyanide. In *Toxicology of Cyanides and Cyanogens: Experimental, Applied and Clinical Aspects*, 1st ed.; Hall, A.H., Isom, G.E., Rockwood, G.A., Eds.; John Wiley & Sons: Chichester, UK, 2015; pp. 82–97. ISBN 978-1119978534.
62. Kunz, D.A.; Nagappan, O.; Silva-Avalos, J.; Delong, G.T. Utilization of cyanide as nitrogenous substrate by *Pseudomonas fluorescens* NCIMB 11764: Evidence for multiple pathways of metabolic conversion. *Appl. Environ. Microbiol.* **1992**, *58*, 2022–2029. [[CrossRef](#)] [[PubMed](#)]
63. Avcioglu, N.H.; Bilkay, I.S. Biological Treatment of Cyanide by Using *Klebsiella pneumoniae* Species. *Food Technol. Biotechnol.* **2016**, *54*, 450–454. [[CrossRef](#)] [[PubMed](#)]
64. Dwivedi, N.; Balomajumder, C.; Mondal, P. Comparative evaluation of cyanide removal by adsorption, biodegradation, and simultaneous adsorption and biodegradation (SAB) process using *Bacillus cereus* and almond shell. *J. Environ. Biol.* **2016**, *37*, 551.
65. Justo Arevalo, S.; Zapata Sifuentes, D.; Cuba Portocarrero, A.; Brescia Reátegui, M.; Monge Pimentel, C.; Farage Martins, L.; Marques Pierry, P.; Morais Piroupo, C.; Guerra Santa Cruz, A.; Quiñones Aguilar, M.; et al. Genomic Characterization of *Bacillus safensis* Isolated from Mine Tailings in Peru and Evaluation of Its Cyanide-Degrading Enzyme CynD. *Appl. Environ. Microbiol.* **2022**, *88*, e0091622. [[CrossRef](#)]
66. Watanabe, A.; Yano, K.; Ikebukuro, K.; Karube, I. Cyanide hydrolysis in a cyanide-degrading bacterium, *Pseudomonas stutzeri* AK61, by cyanidase. *Microbiology* **1998**, *144 Pt 6*, 1677–1682. [[CrossRef](#)]
67. Panay, A.J.; Vargas-Serna, C.L.; Carmona-Orozco, M.L. Biodegradation of cyanide using recombinant *Escherichia coli* expressing *Bacillus pumilus* cyanide dihydratase. *Rev. Colomb. Biotechnol.* **2020**, *22*, 27–35. [[CrossRef](#)]
68. Dursun, A.Y.; Uslu, G.; Cuci, Y.; Aksu, Z. Bioaccumulation of copper(II), lead(II) and chromium(VI) by growing *Aspergillus niger*. *Process Biochem.* **2003**, *38*, 1647–1651. [[CrossRef](#)]
69. Maciel, A.C.; Da Silva Pena, R.; do Nascimento, L.D.; de Oliveira, T.A.; Chagas-Junior, G.C.A.; Lopes, A.S. Health exposure risks and bioremediation of cyanide in cassava processing effluents: An overview. *J. Water Process Eng.* **2023**, *55*, 104079. [[CrossRef](#)]
70. Monga, I.; Paul, V.; Muniyasamy, S.; Zinyemba, O. Green Synthesis of Sodium Cyanide Using Hydrogen Cyanide Extracted under Vacuum from Cassava (*Manihot esculenta* Crantz) Leaves. *Sustain. Chem.* **2022**, *3*, 312–333. [[CrossRef](#)]
71. Shivanoor, S.M.; David, M. Fourier transform infrared (FT-IR) study on cyanide induced biochemical and structural changes in rat sperm. *Toxicol. Rep.* **2015**, *2*, 1347–1356. [[CrossRef](#)]
72. Nandiyanto, A.B.D.; Oktiani, R.; Ragadhita, R. How to Read and Interpret FTIR Spectroscopy of Organic Material. *Indones. J. Sci. Technol.* **2019**, *4*, 97. [[CrossRef](#)]
73. Ojaghi, A.; Shafaie Tonkaboni, S.Z.; Shariati, P.; Doulati Ardejani, F. Novel cyanide electro-biodegradation using *Bacillus pumilus* ATCC 7061 in aqueous solution. *J. Environ. Health Sci. Eng.* **2018**, *16*, 99–108. [[CrossRef](#)] [[PubMed](#)]
74. Razanamahandry, L.C.; Andrianisa, H.A.; Karoui, H.; Kouakou, K.M.; Yacouba, H. Biodegradation of free cyanide by bacterial species isolated from cyanide-contaminated artisanal gold mining catchment area in Burkina Faso. *Chemosphere* **2016**, *157*, 71–78. [[CrossRef](#)]
75. Abouian Jahromi, M.; Jamshidi-Zanjani, A.; Khodadadi Darban, A. Heavy metal pollution and human health risk assessment for exposure to surface soil of mining area: A comprehensive study. *Environ. Earth Sci.* **2020**, *79*, 365. [[CrossRef](#)]
76. Celandroni, F.; Vecchione, A.; Cara, A.; Mazzantini, D.; Lupetti, A.; Ghelardi, E. Identification of *Bacillus* species: Implication on the quality of probiotic formulations. *PLoS ONE* **2019**, *14*, e0217021. [[CrossRef](#)]
77. Durairaju Nisshanthini, S.; Teresa Infanta S, A.K.; Raja, D.S.; Natarajan, K.; Palaniswamy, M.; Angayarkanni, J. Spectral characterization of a pteridine derivative from cyanide-utilizing bacterium *Bacillus subtilis*—JN989651. *J. Microbiol.* **2015**, *53*, 262–271. [[CrossRef](#)]
78. Dangi, A.K.; Sharma, B.; Hill, R.T.; Shukla, P. Bioremediation through microbes: Systems biology and metabolic engineering approach. *Crit. Rev. Biotechnol.* **2019**, *39*, 79–98. [[CrossRef](#)]



79. Luque-Almagro, V.M.; Huertas, M.-J.; Martínez-Luque, M.; Moreno-Vivián, C.; Roldán, M.D.; García-Gil, L.J.; Castillo, F.; Blasco, R. Bacterial degradation of cyanide and its metal complexes under alkaline conditions. *Appl. Environ. Microbiol.* **2005**, *71*, 940–947. [[CrossRef](#)]
80. Satyanarayana, T.; Johri, B.N. *Microorganisms in Environmental Management*; Springer: Dordrecht, The Netherlands, 2012; ISBN 978-94-007-2228-6.
81. Kaspar, F.; Neubauer, P.; Gimpel, M. Bioactive Secondary Metabolites from *Bacillus subtilis*: A Comprehensive Review. *J. Nat. Prod.* **2019**, *82*, 2038–2053. [[CrossRef](#)] [[PubMed](#)]
82. Luque Almagro, V.M. *Metabolismo Del Cianuro y Del Cianato en "Pseudomonas pseudoalcaligenes" CECT5344: Aplicaciones Biotecnológicas: (Accésit)*; Analistas Económicos de Andalucía: Málaga, Spain, 2006; ISBN 978-84-95191-81-6.
83. Botz, M.M.; Mudder, T.I.; Akcil, A.U. Cyanide Treatment. In *Gold Ore Processing*; Elsevier: Amsterdam, The Netherlands, 2016; pp. 619–645. ISBN 9780444636584.
84. Benedik, M.J.; Sewell, B.T. Cyanide-degrading nitrilases in nature. *J. Gen. Appl. Microbiol.* **2018**, *64*, 90–93. [[CrossRef](#)] [[PubMed](#)]
85. Crum, M.A.; Sewell, B.T.; Benedik, M.J. *Bacillus pumilus* Cyanide Dihydratase Mutants with Higher Catalytic Activity. *Front. Microbiol.* **2016**, *7*, 1264. [[CrossRef](#)] [[PubMed](#)]
86. Jandhyala, D.; Berman, M.; Meyers, P.R.; Sewell, B.T.; Willson, R.C.; Benedik, M.J. CynD, the cyanide dihydratase from *Bacillus pumilus*: Gene cloning and structural studies. *Appl. Environ. Microbiol.* **2003**, *69*, 4794–4805. [[CrossRef](#)]
87. Guamán Guadalupe, M.P.; Nieto Monteros, D.A. Evaluation of the rotational speed and carbon source on the biological removal of free cyanide present on gold mine wastewater, using a rotating biological contactor. *J. Water Process Eng.* **2018**, *23*, 84–90. [[CrossRef](#)]
88. Terada, A.; Komatsu, D.; Ogawa, T.; Flamandita, D.; Sahlan, M.; Nishimura, M.; Yohda, M. Isolation of cyanide-degrading bacteria and molecular characterization of its cyanide-degrading nitrilase. *Biotechnol. Appl. Biochem.* **2022**, *69*, 183–189. [[CrossRef](#)]
89. Oudjehani, K.; Zagury, G.J.; Deschênes, L. Natural attenuation potential of cyanide via microbial activity in mine tailings. *Appl. Microbiol. Biotechnol.* **2002**, *58*, 409–415. [[CrossRef](#)]
90. Deloya, A. Tratamiento de desechos del cianuro por biorremediación. *Tecnología en Marcha* **2012**, *25*, 61–72. [[CrossRef](#)]
91. Baxter, J.; Cummings, S.P. The current and future applications of microorganism in the bioremediation of cyanide contamination. *Antonie Van Leeuwenhoek* **2006**, *90*, 1–17. [[CrossRef](#)]

**Disclaimer/Publisher's Note:** The statements, opinions and data contained in all publications are solely those of the individual author(s) and contributor(s) and not of MDPI and/or the editor(s). MDPI and/or the editor(s) disclaim responsibility for any injury to people or property resulting from any ideas, methods, instructions or products referred to in the content.